J. Membrane Biol. 94, 233–243 (1986)

The Journal of
Membrane Biology
© Springer-Verlag New York Inc. 1986

Proton Transport and Membrane Shuttling in Turtle Bladder Epithelium

Troy E. Dixon, Chris Clausen,† Denise Coachman, and Bernard Lane‡
Department of Medicine, VA Medical Center, Northport, New York 11768 and Departments of Physiology and Biophysics† and Pathology,‡ SUNY Health Sciences Center, Stony Brook, New York 11794

Summary. Proton secretion in the urinary bladder of the freshwater turtle is mediated by proton pumps located in the apical membrane of carbonic-anhydrase (CA)-rich cells. It has been proposed that the rate of proton transport is regulated by endocytotic and exocytotic fusion processes which alter the apical membrane area, and hence number of exposed pumps. Three techniques were used to study this process. Analyses of transepithelial impedance provided estimates of transport-associated changes in net membrane area, as well as other electrical parameters. Electron microscopy allowed visualization of the endocytotic vesicles thought to be involved in the process. Finally, uptake of a fluorescent fluid-phase marker provided measurements of the rates of endocytosis. We report the following: (i) endocytotic and exocytotic processes occur primarily in the CA-rich cells; (ii) inhibition of proton transport resulting from 0.5 mM acetazolamide (AZ) results in a decrease in the apical membrane area of approximately 0.47 cm^2/cm^2 tissue; (iii) the apical membrane specific conductance of the CA-rich cells is approximately 220 $\mu S/\mu F$, and possibly represents a Cl^- conductance that may function in counter-ion flow; (iv) the decline in transport following AZ is not directly proportional to the decline in apical membrane area, suggesting that changes in pump kinetics are also involved in the regulation of transport; (v) the CA-rich cells exhibit a high rate of constitutive pinocytosis, and hence membrane shuttling, which appears to be independent of the rate of transport; (vi) AZ induces a transient increase in the rates of endocytosis and shuttling; and (vii) the transport-associated changes in apical membrane area may reflect an effect of AZ on a regulated endocytotic pathway which is distinct from the pinocytotic process.

Key Words proton transport · turtle bladder · equivalent-circuit analysis · impedance analysis · acetazolamide · endocytosis · exocytosis · pinocytosis · membrane shuttling

Introduction

Many details of the process of urinary acidification by the collecting tubule have been derived from studies of proton secretion in the turtle urinary bladder. In this epithelium, proton secretion is an active process carried out by a proton pump located in the apical membrane of the tissue [6, 10]. Several lines of evidence suggest that proton transport is mediated by carbonic-anhydrase (CA)-rich cells, which account for approximately 10 to 20% of the number of cells in the bladder [12, 18]. Although the dependence of transport on the activity of CA has previously been well documented [21, 23], the mechanisms linking the activity of CA to proton transport are not completely understood.

It has previously been shown from electron-microscopic studies that treatment of the bladder with the CA inhibitor acetazolamide (AZ) is associated with a morphological transformation characterized by a reduction of prominent microplicae present on the apical surface of the CA-rich cells [12]. Moreover, using transepithelial impedance-analysis techniques, we have recently reported that AZ causes a reduction of the ionic conductance of the apical membrane of the bladder, which could be completely explained by a reduction in the apical surface area as judged by a decrease in the apical membrane capacitance [2]. These findings raise the possibility that the inhibition of transport by AZ involves changes in the surface area of the apical membrane.

Investigators have recently shown that one mechanism of regulating the rate of proton transport in this epithelium involves changing the number of proton pumps present in the apical membrane of the CA-rich cells [1, 9]. An increase in the number of pumps could be achieved by increasing exocytotic fusion of proton-pump-containing cytosolic vesicles with the apical membrane, or by decreasing the rate of endocytotic removal of apical membrane. Hence, this raises the possibility that the surface-area changes noted following AZ may be indicative of an effect of this agent on the relative rates of endocytosis or exocytosis in the turtle bladder.

The studies presented in this paper were done to investigate further the relationship between

changes in the rate of proton transport and apical membrane electrical characteristics in the turtle bladder in response to AZ. Moreover, we wished to investigate endocytosis and exocytosis and their potential involvement in the regulation of transport in response to AZ.

Materials and Methods

Dissection and Solutions

Freshwater turtles, *Pseudymys scripta elegans*, were double pithed and the urinary bladder excised with a minimal amount of handling. All experiments were carried out at room temperature.

The mucosa and serosa were both bathed in a modified phosphate Ringer's solution having the following composition (in mM): 110 NaCl, 3.5 KCl, 1.0 $MgCl_2$, 1.0 $CaCl_2$, 1.0 Na_2HPO_4, and 5.0 D-glucose. The pH was adjusted to 7.0 and the solutions were bubbled with room air which had been passed through KOH traps to remove CO_2.

Proton transport was inhibited by adding 0.5 mM AZ (Sigma, St. Louis, Mo.) to the serosal solution. In order to test the notion that the effects of AZ result specifically from its inhibitory action on CA, in some experiments we added 0.5 mM t-butyl AZ [2-acetamido-1,3-4-thiadiazole-5-(N-t-butyl)] to the serosal solution. This chemically allied analogue of AZ is inert in regard to proton transport and CA activity [14]. The t-butyl AZ was kindly provided by Dr. T. Maren (Dept. of Pharmacology and Therapeutics, University of Florida College of Medicine, Gainesville, Fla.).

In most experiments, 2% bovine serum albumin (Fraction V, Sigma) was added to the serosal bathing solution [2]. The albumin was omitted from our initial endocytosis experiments since it was thought that it might interfere with the determination of the epithelial protein content. In a subsequent series of experiments, we found this not to be the case, and hence albumin was included in the serosal solution.

Measurements of the Rate of Proton Secretion

The turtle bladder possesses an active Na^+ transport process which results in a mucosa-to-serosa short-circuit (I_{sc}). In all experiments, this transport process was inhibited by the mucosal addition of 0.1 mM amiloride (kindly provided as a gift from Merck, Sharpe and Dohme, Rahway, N.J.). Addition of amiloride causes a reversal of the polarity of I_{sc}, and is sometimes referred to as the reversed short-circuit current, or RSCC. In the presence of total inhibition of Na^+ transport, this current has been shown to be equivalent to the rate of proton secretion [26]. *Rates of proton transport will be referred to as positive values of* I_{sc}, despite the fact that this current is directed from serosa to mucosa. We should note that amiloride sometimes does not result in complete inhibition of Na^+ transport, and hence one can observe a small residual negative I_{sc} after complete inhibition of proton transport.

Transepithelial Impedance Measurements

Hemibladders were mounted in modified Ussing chambers specially designed to eliminate mounting damage [13]. The nominal surface area of the chamber was 2.0 cm^2, and each half-chamber had a volume of 15 ml. The mucosal and serosal solutions were bubbled continuously (*see above*) and gently stirred using magnetic fleas. A small amount of silicon oil (Antifoam A, Dow Corning, Midland, Mich.) was sprayed atop the serosal bath to control foam production resulting from bubbling the albumin-containing solution.

Transepithelial voltage (V_t) was measured differentially using a high-speed high-impedance amplifier (model 113, Princeton Applied Research, Princeton, N.Y.), connected to a pair of Ag-AgCl electrodes mounted close to the preparation. A second set of Ag-AgCl electrodes was mounted at opposite ends of the chamber and used to pass transepithelial current. Constant current was generated using a calibrated 1 MΩ carbon series resistor connected to the mucosal current electrode; the serosal current electrode was connected to ground. I_{sc} was measured intermittently by passing a 500-msec current pulse which depolarized V_t to zero.

Transepithelial impedance was measured using the method of Clausen and Fernandez [3]. A detailed description of the technique can be found in Clausen, Reinach and Marcus [4], and the details of its use in the turtle bladder can be found in Clausen and Dixon [2].

Measurement of the Rate of Endocytosis

The rate of endocytosis was measured by a method described by Reeves, Gluck and Al-Awqati [17]. In these experiments, FITC-dextran was used as a fluid-phase marker, and its uptake by the bladder was used to measure the rate of endocytosis. Paired hemibladders were mounted in modified Ussing chambers with an exposed surface area of 3 cm^2, and mucosal and serosal volumes of 6 ml.

The following experimental protocol was used:

1. The serosal solution was continuously perfused at a rate of 5 ml/min with the phosphate Ringer's solution, and the effluent was collected. The mucosal solution initially contained phosphate Ringer's solution, but was not perfused.

2. The hemibladder was then incubated with mucosal phosphate Ringer's solution containing 50 mg/ml FITC-dextran (70,000 molecular weight, Sigma). Incubation times of 15 min were normally used, but in one series of experiments an incubation time of 45 min was used. The FITC-dextran was previously dialyzed overnight against a phosphate Ringer's solution at zero degrees.

3. Following this incubation, the mucosal solution was removed, and the apical surface of the bladder was washed with 100 ml of ice-cold saline (110 mM NaCl).

4. Following the wash, the apical surface of the bladder was incubated in 2.5 ml of ice-cold 2 N HCl for one minute in order to remove any adherent mucous [16]. The apical surface was again washed with 100 ml of ice-cold saline.

5. The cells were subsequently lysed using 2.5 ml of 0.1% SDS (Sigma) in 25 mM Tris-HCl (pH 8.0). After one minute in this solution, the apical surface was lightly scraped with a metal spatula.

6. The lysate was decanted and mixed by aspiration in a glass pipette in order to ensure dissolution of any membranes present. After allowing any remaining particulate matter to settle, the supernatant was decanted. Its FITC-dextran content was measured using a fluorescence spectrophotometer (model LS-5, Perkin-Elmer, Norwalk, Conn.) at an exciting wavelength of 495 nm and an emission wavelength of 520 nm.

In the majority of experiments, the FITC-dextran content was also measured in a 2.5-ml aliquot of the serosal effluent (total volume *ca.* 75 ml). In 46 out of 53 cases, the increase in serosal

fluorescence was too low to measure. In seven cases, a small increase was measured (0.6 ± 1.1% compared to the apical homogenate) and suggested the presence of a serosal leak due to epithelial mounting damage. To rule out the possibility that the increase in serosal fluorescence was due to transcellular transport of FITC-dextran, we performed a series of experiments utilizing different chambers specifically designed to eliminate edge damage [13]. We consistently observed no measurable increase in serosal fluorescence in 20 experiments using these chambers.

The fluorescent signal of the apical homogenate was converted into a volume of endocytotic fluid by daily constructing standard curves measuring the fluorescence of known volumes of FITC-dextran incubation media in solutions containing Tris-HCl and SDS (*see above*). Finally, after digestion of the hemibladder in 1 N NaOH, its total protein was determined by a protein assay (Bio-Rad Laboratories, Richmond, Calif.). The rate of endocytosis is expressed as volume per unit time per weight of protein, or volume per unit time per cm^2 of tissue.

Validation of the FITC-Dextran Method

Before using the above method for measurement of rates of endocytosis, one must verify that (i) FITC-dextran does not affect proton transport, (ii) FITC-dextran is selectively endocytosed by CA-rich cells, and (iii) the HCl and saline washing procedures remove extracellular marker but do not result in loss of intracellular FITC-dextran. In control experiments, we found that the mucosal addition of 50 mg/ml of FITC-dextran did not affect I_{sc} when the bladder was bathed in phosphate Ringer's solution. In addition, we confirmed the findings of Gluck et al. [9] who showed that FITC-dextran is selectively endocytosed by CA-rich cells. As shown in Fig. 1, incubation of a hemibladder with FITC-dextran led to distinctive staining of a group of cells in the bladder. These same cells were also stained by the pH-sensitive dye 4-methyl-umbellifferone (4MU) in a manner characteristic of CA-rich cells [11]. In hemibladders which were initially bathed in either AZ or t-butyl AZ, the cells which stained positively for FITC-dextran also costained with 4MU in a manner distinctive of CA-rich cells. We should note that following a 15-min incubation with luminal FITC-dextran, uptake of the marker by non-CA-rich cells was routinely found to be negligible. Finally, using fluorescent microscopy, we verified that following the HCl and saline washes, FITC-dextran was retained by the bladder cells whereas extracellular FITC-dextran was adequately removed. Recall that the HCl and saline washes were performed at 0°C to prevent losses of intracellular marker resulting from exocytosis.

Electron Microscopy and Morphometric Analyses

Transmission electron microscopy was performed in hemibladders in order to view endocytotic vesicles. The tissues were incubated for one hour in a mucosal medium containing 0.3% horseradish peroxidase (HRP). Fixation was subsequently performed using a solution containing 1.2% glutaraldehyde and in a 67-mM cacodylate buffer (pH 7.2). The tissues were postfixed in a similar cacodylate buffer solution containing 1.67% OsO_4. Both media also contained 0.05% ruthenium red as an electron-dense extracellular marker. HRP reaction product was produced using the diaminobenzidine technique. The preparations were not stained prior to viewing in order to enhance the effective contrast of HRP reaction product and ruthenium red. Further details of the methodology can be found in ref. [15].

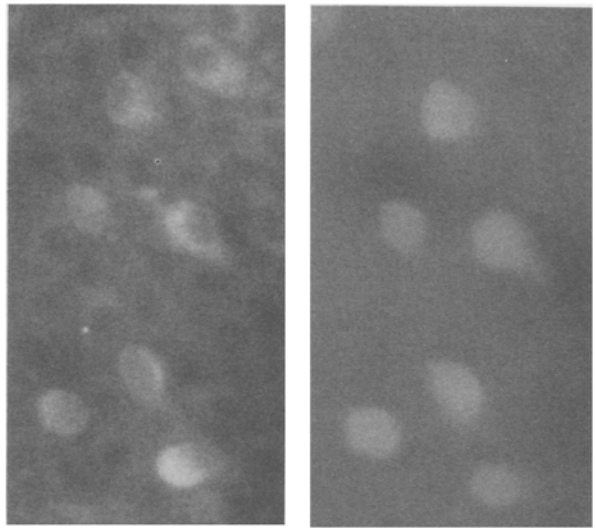

Fig. 1. Fluorescence micrographs (magnification 2000×) of a hemibladder preparation that was incubated with 50 mg/ml FITC-dextran in the mucosal solution, and 0.25 mM 4MU in the serosal solution. The pattern of fluorescence in the left panel (exciting wavelength of 490 nm) shows that FITC-dextran is taken up selectively by a population of cells. The right panel (exciting wavelength of 365 nm) shows that these same cells stain distinctively with the pH-sensitive dye 4MU in a manner that is characteristic of CA-rich cells

The surface area-to-volume ratio of endocytotic vesicles present in the cytoplasm of CA-rich cells was determined by analyzing electron micrographs. Standard stereological point-counting techniques were used and are described in detail in ref. [29]. Briefly, we overlayed each micrograph (magnification of 25,000 to 62,500 diameters) with a 3-mm rectangular grid, and then counted the number of grid intersections that were contained within vesicle boundaries, and the number of grid line intersections that crossed into and out of the vesicles. Using standard formulas [29], we then computed ratios of vesicle volume (V_v) and surface area (S_v) normalized by the effective volume overlayed by the grid. Since in some cases the grid overlayed extracellular space and/or granular cells (which are devoid of endocytotic vesicles), V_v and S_v do *not* represent vesicle volume and surface densities normalized to the volume of CA-rich cells, and hence these values alone are of limited usefulness. However, their ratio (S_v/V_v) equals the vesicle surface area-to-volume ratio which is useful for comparing rates of endocytosis determined from FITC-dextran uptake with net changes in apical membrane area determined from impedance analysis. We should note that the stereological analysis results in area-to-volume ratios which are independent of vesicle geometry.

Results

Results from Impedance Analyses

Impedance-analysis techniques allow one to measure the apical and basolateral membrane conductances (G_a and G_b, respectively). These conductances are proportional to the membrane ionic

Table 1. Results of inhibiting proton transport using 0.5 mM AZ in six hemibladders[a]

	I_{sc} (μA/cm^2)	G_a (mS/cm^2)	C_a (μF/cm^2)	$G_{a\text{-norm}}$ (μS/μF)	G_b (mS/cm^2)	C_b (μF/cm^2)	$G_{b\text{-norm}}$ (μS/μF)	R_p (Ωcm^2)
Control	6.3 ± 1.0	0.23 ± 0.02	3.0 ± 0.4	82 ± 6	3.8 ± 0.7	7.7 ± 0.6	490 ± 90	232 ± 48
0.5 mM AZ	−1.1 ± 0.8	0.14 ± 0.01	2.5 ± 0.3	59 ± 8	3.6 ± 0.7	7.4 ± 0.6	480 ± 100	245 ± 58
$\bar{\Delta}$	7.4 ± 0.6	0.09 ± 0.01	0.47 ± 0.1	22 ± 2	0.2 ± 0.1	0.29 ± 0.3	10 ± 20	12 ± 11
P	0.0001	0.0009	0.005	0.0003	0.1	0.2	0.4	0.2

[a] The first two rows show mean values (± SEM) in the control state and after addition of AZ, respectively. The third row shows the mean difference between the two conditions. The fourth row shows probabilities based on a paired t-test, comparing the control with the AZ-treated state.

permeabilities, but they are also proportional to the membrane areas. Measurements of the membrane areas are needed in order to determine whether changes in conductance result simply from area changes (caused by exocytosis or endocytosis), or whether they reflect changes in membrane specific conductance (conductance per unit area) thereby reflecting changes in ionic permeability.

Impedance-analysis techniques also allow one to measure the apical and basolateral membrane capacitances (C_a and C_b, respectively). Membrane capacitance appears to be proportional solely to membrane area, since nearly all biological membranes exhibit a specific capacitance of approximately 1.0 μF/cm^2 [5]. Hence, these measurements not only allow one to quantify membrane area changes resulting from endocytosis and exocytosis, but they also allow one to estimate the membrane specific conductances by normalizing G_a and G_b to unit area (i.e., $G_{a\text{-norm}} = G_a/C_a$ and $G_{b\text{-norm}} = G_b/C_b$).

Finally, the turtle bladder possesses narrow lateral space (*ca.* 10 nM) which result in a significant resistance in series with the basolateral membrane and distributed along the lateral spaces. We showed previously that this resistance (R_p) can be determined using the impedance analysis technique if one uses a suitable equivalent-circuit model of the epithelium [2]. R_p is proportional to the resistivity of the lateral-space bathing solution, and is inversely proportional to the width of the lateral spaces. Procedures which cause cell swelling are expected to result in narrowing of the lateral spaces thereby increasing R_p.

Effect of AZ on Membrane Electrical Characteristics

We have previously reported that 50 μM AZ results in a significant decline in proton transport amounting to a 71% reduction in I_{sc} measured under control (phosphate Ringer's) conditions. This was accompanied by changes in the membrane electrical characteristics measured using transepithelial impedance-analysis techniques [2]. Namely, we found that 50 μM AZ resulted in a decrease in G_a which could be fully explained by a concomitant decline in C_a (hence, apical membrane area), since it occurred without a change in the $G_{a\text{-norm}}$. No significant changes were observed in G_b, C_b or R_p.

In these earlier studies, we also found that both the decline in transport and the decline in C_a resulting from 50 μM AZ could be readily reversed by stimulating transport with serosal bicarbonate Ringer's solutions. In these studies, use of a reversible dose of AZ was important in the validation of the impedance technique. In the present studies, we decided to use a higher dose of AZ (0.5 mM) in order to produce maximal changes in proton transport. Although 0.5 mM AZ inhibits proton transport irreversibly, we anticipated that the changes in membrane electrical parameters would be greater, thus allowing better analysis of the details of the changes.

As shown in Table 1, changing the serosal solution from a control phosphate Ringer's to one containing 0.5 mM AZ caused a complete inhibition of I_{sc} from a control value of 6.3 to −1.1 μA/cm^2 (this small negative current probably reflects residual Na^+ transport). This amounted to a significantly greater degree of inhibition ($P = 0.02$, unpaired t-test) than was observed earlier with 50 μM AZ. Similar to the findings with the lower dose, we found that 0.5 mM AZ resulted in a significant decline in G_a and in C_a, but the decline in C_a (16 ± 3%) was significantly greater ($P = 0.02$) that than observed following 50 μM AZ. In contrast to our findings with the lower dose, 0.5 mM AZ resulted in a significant reduction in $G_{a\text{-norm}}$ thereby suggesting a reduction in the apical membrane specific conductance and hence ionic permeability. No significant changes were observed in G_b, C_b or R_p resulting from 0.5 mM AZ, indicating that its electrophysiological effects are specific to the apical membrane.

Time Course of the Changes in Apical-Membrane Parameters

Our transport-related changes in C_a are consistent with electron-microscopic studies [12] which show that AZ causes a decline in apical-membrane surface area in the CA-rich cells. Given the recent data of Gluck et al. [9] which suggest that the rate of proton transport in the turtle can be regulated by the exocytotic fusion of proton-pump-containing vesicles with the apical membrane, or by the endocytotic removal of apical membrane, we thought it possible that the decline in surface area noted following AZ treatment might reflect alterations of the rates of these processes. If this were the case, then comparison of the time courses of the decline in I_{sc} and the decline in C_a should support this notion.

Figure 2 shows I_{sc}, C_a, and $G_{a\text{-norm}}$ measured from a single representative hemibladder and plotted as a function of time. Changing the serosal solution to one containing 0.5 mM AZ results in a decline in both I_{sc} and C_a which begin simultaneously. However, the decline in I_{sc} is not found to be entirely correlated with the decline in C_a. I_{sc} rapidly declines over the first 24 min following AZ, corresponding to an 18-μA decrease per μF decrease in C_a. Shortly thereafter, transport is abolished but C_a continues to decrease. We should note that washing the serosal solution with AZ-free bicarbonate Ringer's solution (*see* legend, Fig. 2) failed to restore I_{sc} and C_a to control levels, verifying that 0.5 mM AZ acts irreversibly.

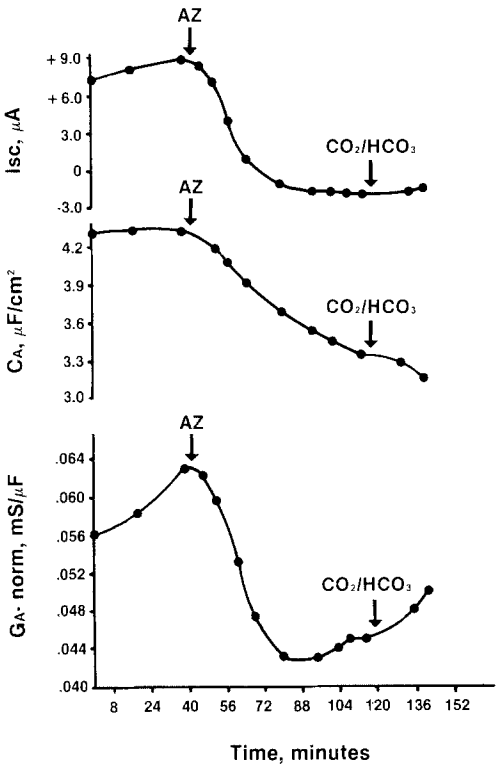

Fig. 2. I_{sc}, C_a and $G_{a\text{-norm}}$ measured as a function of time in a representative hemibladder. At the point marked AZ, 0.5 mM AZ was added to the serosal solution. Note that C_a continued to decline following complete inhibition of transport. At the point marked CO_2/HCO_3^-, the serosa was changed to an AZ-free Ringer's solution that was modified to contain 100 mM NaCl and 10 mM $NaHCO_3$, and was bubbled with air containing 5% CO_2. This maneuver failed to restore transport, and illustrates that 0.5 mM AZ acts irreversibly

Endocytosis

The electrophysiological data just presented suggest that the observed changes in C_a with transport are mediated by endocytosis and/or exocytosis of apical membrane. In order to quantify endocytosis, we measured intracellular uptake of FITC-dextran. Under control conditions, we found a baseline rate of endocytosis equal to 0.64 ± 0.15 nl/min/mg protein (n = 7), or 0.46 ± 0.05 nl/min/cm^2 tissue.[1] Both these calculations assume that the concentration of FITC-dextran in the endocytotic vesicles is the same as that in the mucosal bulk solution. We have previously shown that hemibladders bathed under identical conditions exhibited a stable apical membrane capacitance, implying a constant apical membrane area. From these results, we conclude that there is a continual recycling of apical membrane involving a shuttling mechanism in which baseline endocytosis and exocytosis proceed at equivalent rates.

As a test of our assertion of a continual shuttling of apical membrane, we analyzed electron micrographs of hemibladders in an attempt to observe intracellular localization of HRP, a different fluid phase marker. Figure 3 shows a micrograph of the apical side of a hemibladder incubated with HRP for one hour under control conditions. One clearly observes intracellular vesicles which have been labeled with HRP reaction product only in cells with prominent microplicae, a morphological characteristic of CA-rich cells [12, 28]. Hence these results further support the notion of a continuous baseline rate of endocytosis.

[1] This rate of endocytosis was measured from bladders incubated with FITC-dextran for 45 min. In hemibladders incubated for 15 min, we measure a mean baseline rate of endocytosis of 0.66 ± 0.06 nl/min/mg protein (n = 47), a value which is indistinguishable from the rate measured using the longer incubation time (P = 0.5). This suggests that FITC-dextran uptake is linear and does not saturate over a 45-min period.

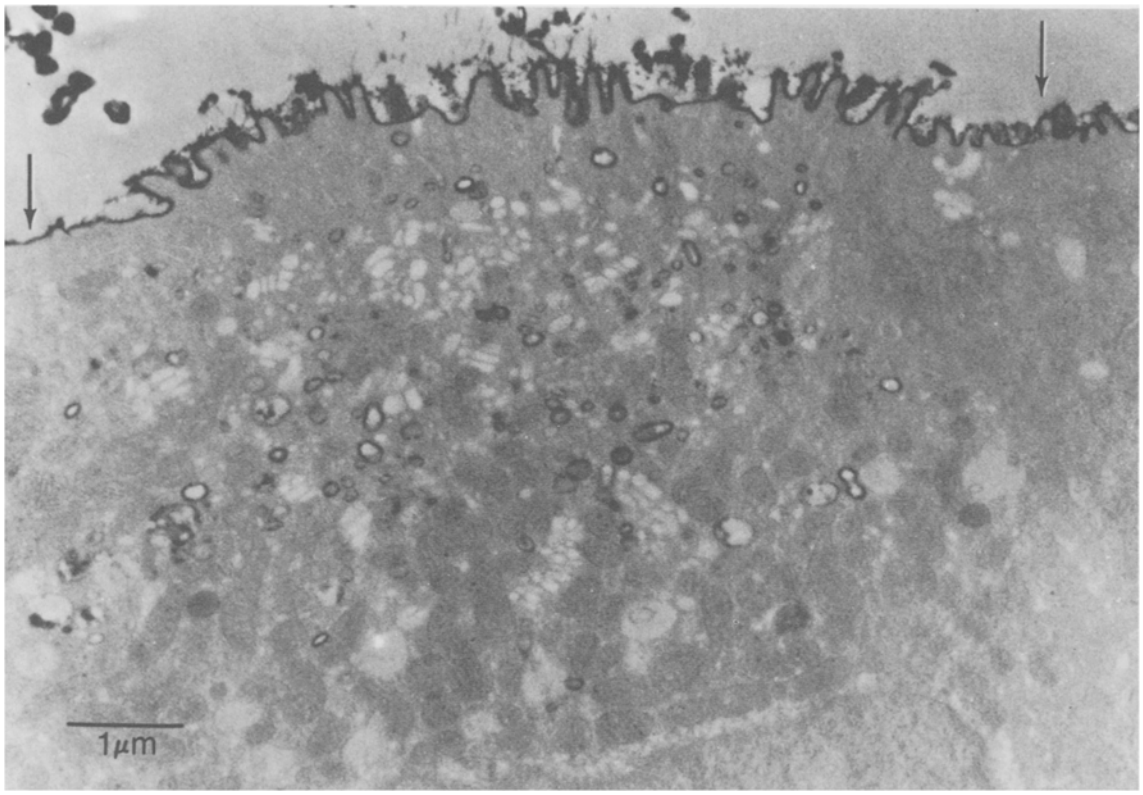

Fig. 3. Electron micrograph showing a cell with prominent apical membrane microplicae characteristic of the α-type CA-rich cells. Also seen are portions of bordering cells exhibiting more planar apical membranes (arrows), which are characteristic of granular cells. Prior to fixation, the hemibladder was bathed with a solution containing HRP. During fixation, the solution contained ruthenium red. Observe the intracellular vesicles that show electron-dense HRP reaction product. The micrograph is from an unstained preparation

For purposes of comparing our measured rates of baseline shuttling with those reported in other tissues, it is useful to normalize the rate of endocytosis to cell volume and apical membrane area. It has previously been reported that the hemibladder cells contain approximately 4.2 μl cell water per mg cell protein [7], and that the CA-rich cells account for approximately 10 to 20% of the total cell number [12]. If we assume that all cells contain approximately the same amount of cell water relative to protein content, then we calculate that the uptake of fluid amounts of approximately 0.08 to 0.2% of the cell volume each minute.

In order to calculate the rate of membrane turnover requires estimates of the average area-to-volume ratio of the vesicles in the CA-rich cells, and this was determined using stereological point-counting techniques. We analyzed five electron micrographs obtained from a total of four different hemibladders. Our analysis was restricted to 227 vesicles that were located within 5 μm of the apical membrane. The majority of these vesicles were clearly labeled with HRP reaction product, but a few (<10%) were unlabeled but in close proximity to labeled vesicles. A statistical analysis (*see* ref. 29) allowed us to estimate the precision in our estimates of S_v and V_v for each of the micrographs. The mean accuracy in the determination of S_v and V_v was 9.5% (range 8 to 13%) and 11% (range 6 to 17%), respectively.

We obtained a mean value of the vesicle surface area-to-volume ratio of $2.8 \pm 0.2 \times 10^5$ cm^2/cm^3, and from this we calculate a turnover of apical membrane of 0.13 cm^2/min/cm^2 tissue. Finally, the value for C_a (Table 1) indicates that the total epithelial surface area is approximately 3 cm^2/cm^2 tissue, and micrographic estimates of relative cell number and apical membrane amplification [27] indicate that roughly 30% of this area is accounted for by the CA-rich cells. Hence the amount of membrane that is shuttled each minute is equivalent to nearly 15% of the CA-rich cell apical membrane area.

Effect of AZ on Rates of Endocytosis

The rates of endocytosis were measured in paired hemibladders after the addition of 0.5 mM AZ to

Table 2. Endocytotic uptake of FITC-dextran following application of 0.5 mM serosal AZ[a]

Time period		FITC-dextran uptake (nl/min/mg protein)		
	n	Control	Experimental	*P*
0 to 15 min after AZ	6	0.67 ± 0.21	0.86 ± 0.25	0.24
15 to 30 min after AZ	12	0.65 ± 0.09	1.11 ± 0.23	0.03
75 to 90 min after AZ	7	0.90 ± 0.20	0.88 ± 0.15	0.43
15 to 30 min after t-butyl AZ	5	0.69 ± 0.29	0.80 ± 0.36	0.19

[a] The column labeled Control is the mean uptake rate (± SEM) in the control hemibladder, and the column labeled Experimental is the corresponding rate in the paired AZ-treated hemibladder. The column labeled *P* is the probability, based on a paired *t*-test, comparing the two states. For the 0 to 15 min period, I_{sc} decreased from 11 ± 1 to 3.3 ± 1.0 μF/cm^2. For the 15 to 30 min period, I_{sc} decreased from 3.9 ± 0.6 to 0.83 ± 0.44 μA/cm^2. I_{sc} was essentially zero throughout the 75 to 90 min period. The last row shows that t-butyl AZ has no effect on the rate of endocytosis.

each experimental hemibladder[2], and the results of these experiments are shown in Table 2. In the first 15 min following application of AZ, the rate of transport decreased by 69%, but no difference in the rate of endocytosis was noted. In the 15- to 30-min period, transport declined to near zero, and the rate of endocytosis nearly doubled. Finally, after total inhibition of transport (75 to 90 min after application of AZ), the rate of endocytosis was found to be indistinguishable from the control rate ($P > 0.8$, unpaired *t*-test). A chemically allied AZ derivative, t-butyl AZ, lacks the ability to inhibit CA and had no effect ($P > 0.8$) on either proton transport or the rate of endocytosis.

We conclude that inhibition of transport with AZ produces a transient increase in the rate of endocytosis which is specifically related to the ability to AZ to inhibit CA activity. Although in the first 15 min after application of AZ we find a significant decline in transport and no significant change in the rate of endocytosis, we do not believe that this truly represents a dissociation between the processes. We suspect that the inability to observe a change in the rate of endocytosis during this initial time period simply reflects poor time resolution of the method. This most likely results from the time required for FITC-dextran to cross the mucosal unstirred layer, coupled to the time lag (*ca.* 5 min, or one-third the FITC-dextran incubation period) between the serosal addition of AZ and a noticeable decrease in I_{sc} and C_a.

[2] In this series of experiments, the hemibladders were maintained in the short-circuited state, and the serosal solution did not contain albumin. The control rates of endocytosis did not differ significantly ($P = 0.3$, unpaired *t*-test) from hemibladders bathed in a serosal solution containing albumin, and maintained under open-circuit conditions.

Effects of AZ on Membrane Shuttling

The results presented so far show that the application of AZ causes a transient increase in the rate of endocytosis, as well as a net decrease in the apical membrane area as reflected by a decrease in C_a. In the baseline state, we found a continual shuttling of apical membrane in which the rates of endocytosis and exocytosis were equivalent. In view of this, we wanted to determine whether AZ solely affects the rate of endocytosis, or whether the rate of exocytosis (and hence shuttling) is altered as well.

The application of AZ results in a 0.47 μF/cm^2 decrease in C_a (Table 1) that is complete within *ca.* 45 min. Assuming that the specific capacitance of the apical membrane is 1 μF/cm^2, then this would indicate that AZ results in the internalization of apical membrane amounting to 0.47 cm^2/cm^2 tissue. If AZ results solely in an increase in the rate of endocytosis, then the increase in volume uptake of FITC-dextran should account for the decrease in apical membrane area.

We measured FITC-dextran uptake over 45 min in 7 paired hemibladders mounted under identical conditions as the impedance studies. One member of each pair was treated with 0.5 mM AZ, and the other served as a control. AZ induced a significant increase in FITC-dextran uptake of 9.4 ± 4.0 nl/cm^2 ($P = 0.03$) compared to the control level. Using the vesicle surface area-to-volume ratio (*see above*), this uptake corresponds to a membrane area uptake of 2.6 cm^2/cm^2 tissue. Since this value is more than fivefold higher than the net decrease in surface area determined from C_a, this result indicates that the increase in endocytosis is also accompanied by a transient increase in the rate of exocytosis, and hence shuttling.

Discussion

Cellular Heterogeneity

The turtle bladder possesses two major cell types, granular cells which are thought to be responsible for Na^+ transport, and CA-rich cells which are thought to mediate proton transport. Recently, Stetson and Steinmetz [28] presented evidence indicating that in fact the population of CA-rich cells can be further subdivided into two distinct populations: α cells which mediate proton transport, and β cells which mediate HCO_3^- transport. Thus due to this heterogeneity, one must be cautious that the changes in the transport parameters noted in this study truly represent changes occurring in the cell type of intersect.

Clausen and Dixon [2] provided evidence that the transepithelial impedance studies yielded electrical parameters representative of the combined properties of the different cells. Importantly, they showed that maneuvers that are expected to affect specifically the CA-rich cells and proton transport resulted in changes of impedance-determined parameters which compared favorably to the expected changes obtained from morphological studies. Moreover, we verified that the endocytosis of FITC-dextran was specific to CA-rich cells, as determined by fluorescent microscopy. We also showed that endocytosis *per se* was specific to CA-rich cells, as determined by electron microscopic studies involving HRP uptake. Finally, AZ has been shown to affect only the CA-rich cells, since in isolated cells, it reduces the rates of metabolism only in CA-rich cells [22], and since it causes morphological transformations only in cells with prominent microplicae, a characteristic of the α-type CA-rich cells [12, 28]. Therefore, we feel that the values determined in this study regarding rates of endocytosis and alterations of membrane area reflect properties specific to the CA-rich cells.

Membrane Electrical Parameters

In Table 1, we showed that inhibition of transport with 0.5 mM AZ resulted in changes of the electrical properties of only the apical membrane. The resulting decrease in C_a is supported by morphological data which show a decrease in the apical membrane area of the CA-rich cells. Although a concomitant decrease in G_a would also be expected due to this decrease in exposed membrane, the measured decrease in $G_{a\text{-norm}}$ is unexpected since this is a measure of the specific conductance of the apical membrane. There are three possibilities to explain this apparent AZ-dependent decrease in $G_{a\text{-norm}}$: an AZ-induced decrease in the apical membrane permeability of the CA-rich cells, a change in the net electrochemical gradients across the apical membrane of the CA-rich cells, or different specific conductances of the apical membranes of the granular and CA-rich cells.

We find no reported evidence in other tissues that AZ decreases membrane ionic permeability, indicating that it does not block conductive channels. Furthermore, t-butyl AZ, a closely related derivative of AZ, has no effect on transport in turtle bladder, and this would not be expected if AZ-related compounds blocked ionic channels. Finally, even though AZ is known to reduce proton pump activity, either directly or indirectly, this would not be expected to alter the measured specific conductance [2]. The impedance analysis only produces small (*ca.* $\pm$ 5 mV) membrane voltage perturbations which are not expected to alter measurably the pump currents.

We cannot discount the possibility that AZ results in changes in the net electrochemical gradients across the apical membrane. AZ has been shown to increase intracellular pH [24], and this is expected to result in an increase in intracellular HCO_3^-. In addition, the basolateral membrane of the CA-rich cells are known to possess a $Cl^- - HCO_3^-$ exchange process [8], and hence an increase in intracellular HCO_3^- would also be expected to increase intracellular Cl^-. However, if the apical membrane of the CA-rich cells exhibited a permeability to HCO_3^- [19] and/or Cl^-, then an increase in the intracellular activities of these ions would be expected to increase, not decrease, the membrane's specific conductance [20]. We therefore find it unlikely that the decrease in $G_{a\text{-norm}}$ can be explained solely by alterations in intracellular ionic composition. AZ is expected to change the apical transmembrane potential resulting from changes in intracellular composition, and/or from changes in electrogenic pump activity. If the apical membrane possesses a nonlinear I/V relationship, then these changes could alter $G_{a\text{-norm}}$, but it is difficult to predict whether $G_{a\text{-norm}}$ would increase or decrease.

We suspect that the AZ-induced decrease in $G_{a\text{-norm}}$ results from different specific conductances of the apical membranes of the CA-rich and granular cells. In our studies, G_a and C_a reflect the combined conductances and capacitances of the two cell types [2], hence $G_{a\text{-norm}}$ represents a weighted average of the apical specific conductances of the two cell types. Given this information, it becomes clear that a selective decrease in the amount of exposed apical membrane of the CA-rich cells would lead to a value of $G_{a\text{-norm}}$ which more closely ap-

proximates the specific conductance of the granular cells. Since $G_{a\text{-norm}}$ decreased from 82 to 59 μS/μF after AZ, we conclude that specific conductance of the CA-rich cells is higher than that of the granular cells, and that the specific conductance of the granular cells must be less than 59 μS/μF. Moreover, assuming that AZ does not alter the specific conductances of either cell type (*see above*), the absolute changes in G_a and C_a (ΔG_a and ΔC_a) following AZ can be used to estimate the apical membrane specific conductance of the CA-rich cells. This value is calculated as $\Delta G_a/\Delta C_a$ and equals 220 ± 50 μS/μF. We should note that in these studies, the granular cells are expected to exhibit a low apical membrane conductance since Na^+ transport was inhibited with 0.1 mM mucosal amiloride.

It is interesting to note that the apical membrane specific conductance of the CA-rich cells appears to be independent of the dose of AZ. The above value of 220 μS/μF was determined from tissues treated with 0.5 mM AZ. In our earlier study where transport was inhibited using 50 μM AZ [2], we reported decreases in G_a and C_a (ΔG_a and ΔC_a) of 40 μS/cm^2 and 0.2 μF/cm^2, respectively, and from these values we calculate a specific conductance of 200 μS/μF. Note that in these earlier studies using 50 μM AZ, we found that the resulting decrease in $G_{a\text{-norm}}$ was not significant ($P = 0.08$). We now suspect that the failure to observe a significant decrease simply reflects smaller relative changes of apical membrane area. We have no reason to believe that the action of AZ is qualitatively different at the different doses.

It is unclear at this time as to the significance of the apparent apical membrane conductance of the CA-rich cells. We suspect that it represents a Cl^--conductance that might function in counter-ion transport when the bladder is under open-circuit (e.g., *in vivo*) conditions. The available reports on the effect of Cl^- on proton transport were done under short-circuit conditions [8] and also did not address the possible role of the apical membrane Cl^--conductive pathway. Hence further studies are required to investigate this issue.

Time Course of Transport Inhibition

The regulation of proton transport in turtle bladder is thought to involve, at least in part, alterations in apical membrane area. However, studies to date have been unable to follow the time course of this process. We hoped to be able to correlate the decrease in apical membrane area, as reflected in C_a, with the decrease in I_{sc} following inhibition of transport with AZ.

We consistently observed that following treatment with 0.5 mM AZ, the decline in proton transport and the fall in C_a begin at approximately the same time, and this would be expected if the decline in proton transport was regulated by removal of proton-pump containing vesicles. However, we found that after complete inhibition of transport, C_a continued to decline, indicating that the regulation of the rate of transport may not be solely dependent on changes of apical membrane area. In interpreting these results, one can consider two basic factors which may contribute to the regulation of transport following AZ: the number of functioning pumps, and the activity of each individual pump. We can then speculate on at least two possibilities to explain the apparent dissociation between the declines in I_{sc} and C_a.

The decline in transport may involve removal of membrane which contains varying densities of proton pumps. This leads one to postulate that during the early phase of reduction of transport, regions of apical membranes possessing a high density of pumps are selectively endocytosed, and during the later stages of inhibition, the membrane being removed is relatively devoid of pumps. It has been shown that all the endocytotic vesicles are acidic [9], suggesting the presence of proton pumps, but this alone does not provide evidence of a distribution of vesicles possessing different numbers of pumps.

Alternatively, the rate of proton transport may be influenced not only by changes in the number of pumps, but also by changes in the kinetics of the individual pumps. The early phase of inhibition may involve a decrease in the activity of the pumps resulting from changes in factors such as intracellular pH. Concomitant with the reduction in activity, there could occur an increase in endocytotic removal of membrane containing the pumps. The increased endocytosis could be triggered by the same factor(s) which alter pump activity and merely exhibit a different time course than the effect on transport. Alternatively, factors that are related to the activity of the pumps, such as the membrane potential, could provide the signal for increased endocytosis.

Endocytosis and Exocytosis

We measured a significant baseline rate of endocytosis under control conditions that was localized in the CA-rich cells. Under these conditions, C_a remained stable, indicating that the endocytotic process must be coupled to an equivalent rate of exocytosis. This describes an apical membrane shuttling

process occurring under baseline conditions. We should note that Gluck et al. [9] have previously suggested the existence of membrane recycling, and our results are consistent with their findings.

We suspect that this shuttling process represents continual pinocytotic activity of the CA-rich cells. We came to this conclusion by considering two sources of information. First, the size of the vesicles in the CA-rich cells is similar to that of pinocytotic vesicles found in other cells. For example, we measure a mean vesicle area-to-volume ratio of 2.8×10^5 cm^2/cm^3, and in macrophages [25] we calculate a pinocytotic vesicle area-to-volume ratio of 2.2×10^5 cm^2/cm^3 (assuming spherical geometry). Second, the rate of cell volume turnover in the Ca-rich cells amounts to 0.08 to 0.2%/min, which is comparable to rates of 0.07 to 0.4%/min measured in other cells exhibiting pinocytosis [25]. We should note that our estimates of the rates of pinocytosis were determined solely from apical membrane uptake of FITC-dextran, and amounts to a recycling rate of about 15% of the apical membrane area each minute. Although this rate of membrane turnover appears to be significantly higher than that measured in other cells exhibiting pinocytosis (1 to 3%/min, ref. 25), those rates were calculated for the entire cell and in addition are not normalized by cell size. Hence the absolute rates of membrane turnover per cell may in fact be comparable.

The question that now must be addressed is whether or not this pinocytotic process in the CA-rich cells is intimately involved in transport. We can dismiss the possibility that proton transport is mediated by mucosal release of acidic intravesicular contents for two major reasons. First, proton transport is known to be electrogenic. Second, although the vesicles are known to be acidic (*ca.* pH 5, ref. 9), in order to account for the measured rates of transport, the vesicle turnover rate would have to be over six orders of magnitude greater than that which is measured.

Following inhibition of transport with AZ, we observe a decrease in C_a and hence apical membrane area. This is mediated by a transient increase in endocytosis, peaking 15 to 30 min after AZ. The increase in the rate of endocytosis amounted to a membrane area uptake that far exceeded the measured decrease in apical membrane area. Therefore, the increase in endocytosis must be accompanied by an increase in exocytosis, and hence shuttling. After complete inhibition of transport, apical membrane area stabilizes at a lower value, and the rate of endocytosis returns to the baseline value. Thus, the net effect of inhibition of transport with AZ is a transient, not sustained, increase in the rates of endocytosis and shuttling.

Since the rates of shuttling in the baseline and inhibited states were the same, we conclude that this process is independent of the rate of transport, and independent of the apical membrane surface area. Given the current notion that transport is in part regulated by changes in the apical membrane area, and hence number of pumps, then the key variable to consider is the AZ-induced change in apical membrane area, regardless of the rate of shuttling. One of the hallmarks of pinocytosis is that the process occurs without changes in surface area [25], implying a near perfect coupling between the rates of endocytosis and exocytotis. Hence, the transport-dependent decrease in apical membrane area may reflect participation of a regulated endocytotic process that is different than the pinocytotic pathway. If this is the case, the AZ must have effects not only on the regulated endocytotic process, but also must result in stimulation of the rate of pinocytosis, since the calculated rate of internalization of apical membrane far exceeds the measured decrease in apical membrane area. Note, however, that we cannot rule out the possibility that the response to AZ is mediated by uncoupling of the endocytotic and exocytotic components of the pinocytotic pathway.

Conclusions

This study utilized three different methods, analysis of transepithelial impedance, electron microscopy, and uptake of FITC-dextran, to investigate the association of membrane fusion processes and proton transport in turtle bladder. The impedance analyses resulted in measurements of membrane electrical parameters, notably net changes in membrane capacitances which reflect net changes in membrane surface areas. Electron and fluorescence microscopy showed that the endocytotic processes thought to be responsible for transport-associated changes in apical membrane area were localized to the CA-rich cells which are thought to be responsible for proton transport. Measurements of uptake of FITC-dextran yielded the rates of volume uptake by endocytosis. Finally, morphometric analyses of electron micrographs provided the ability to correlate quantitatively the changes in membrane surface area with the rate of endocytosis.

The results obtained are compatible with the notion that the rate of proton transport may be regulated by changes in membrane surface area, and hence number of proton pumps. However, the

results also show that changes in membrane area are not the sole regulatory factor, and suggest that changes in individual pump kinetics contribute as well. Finally, we demonstrate the presence of a continual constitutive pinocytotic process whose function in regard to proton transport is currently unknown.

This work was supported by a Veterans Administration Merit Review Grant, and by National Institutes of Health grants AM-30394 and AM-28074. T.E.D. was a Research Associate of the Veterans Administration while some of these studies were in progress. We also thank Ms. P. Crutchfield for technical assistance in the preparation of micrographs.

References

1. Cannon, C., Adelsberg, J. van, Kelly, S., Al-Awqati, Q. 1985. CO_2-induced exocytotic insertion of H^+ pumps in turtle-bladder luminal membrane: Role of cell pH and calcium. *Nature (London)* **314:**443–446
2. Clausen, C., Dixon, T.E. 1986. Membrane electrical parameters in turtle bladder measured using impedance-analysis techniques. *J. Membrane Biol.* **92:**9–19
3. Clausen, C., Fernandez, J.M. 1981. A low-cost method for rapid transfer function measurements with direct application to biological impedance analysis. *Pfluegers Arch.* **390:**290–295
4. Clausen, C., Reinach, P.S., Marcus, D.C. 1986. Membrane transport parameters in frog corneal epithelium measured using impedance analysis techniques. *J. Membrane Biol.* **91:**213–225
5. Cole, K.S. 1972. Membranes, Ions and Impulses. p. 12. University of California Press, Berkeley, California
6. Dixon, T.E., Al-Awqati, Q. 1979. Urinary acidification is due to a reversible proton translocating ATPase. *Proc. Natl. Acad. Sci. USA* **76:**3135–3138
7. Dixon, T.E., Al-Awqati, Q. 1980. H^+/ATP stoichiometry of proton pump of turtle urinary bladder. *J. Biol. Chem.* **255:**3237–3239
8. Fischer, J.L., Husted, R.F., Steinmetz, P.R. 1983. Chloride dependence of the HCO_3 exit step in urinary acidification by the turtle bladder. *Am. J. Physiol.* **245:**F564–F568
9. Gluck, S., Cannon, C., Al-Awqati, Q. 1982. Exocytosis regulates urinary acidification in turtle bladder by rapid insertion of H^+ pumps into the luminal membrane. *Proc. Natl. Acad. Sci. USA* **79:**4327–4331
10. Gluck, S., Kelly, S., Al-Awqati, Q. 1982. The proton transporting ATPase responsible for urinary acidification. *J. Biol. Chem.* **257:**9230–9233
11. Graber, M.L., Dixon, T.E., Coachman, D., Herring, K., Ruenes, A., Gardener, T., Pastoriza, E. 1986. Fluorescence identifies an alkaline cell in turtle urinary bladder. *Am. J. Physiol.* **250:**F159–F168
12. Husted, R.F., Mueller, A., Kessel, R., Steinmetz, P.R. 1981. Surface characteristics of carbonic anhydrase rich cells in turtle urinary bladder. *Kidney Int.* **19:**491–502
13. Lewis, S.A., Eaton, D.C., Clausen, C., Diamond, J.M. 1977. Nystatin as a probe for investigating the electrical properties of a tight epithelium. *J. Gen. Physiol.* **70:**427–440
14. Maren, T.H. 1956. Carbonic anhydrase inhibition V. N^5-substituted 2-acetylamino-1,3,4-thiadiazole-5-sulfonamides. Metabolic conversion and use as control substances. *J. Pharmacol. Exp. Ther.* **117:**385–393
15. Masur, S.K., Cooper, S., Rubin, M.S. 1984. Effect of an osmotic gradient on antidiuretic hormone-induced endocytosis and hydrosmosis in the toad urinary bladder. *Am. J. Physiol.* **247:**F370–F379
16. Parson, C.L., Mulholland, S. 1978. Bladder surface mucin. *Am. J. Pathol.* **93:**423–432
17. Reeves, W., Gluck, S., Al-Awqati, Q. 1983. Role of endocytosis in H^+ secretion. *Kidney Int.* **23:**237
18. Rosen, S. 1972. Localization of carbonic anhydrase activity in turtle and toad urinary bladder mucosa. *J. Histochem. Cytochem.* **20:**696–702
19. Satake, N., Durham, J.H., Ehrenspeck, G., Brodsky, W.A. 1983. An electrogenic mechanism for alkali and acid transport in turtle bladders. *Am. J. Physiol.* **244:**C259–C269
20. Schultz, S.G. 1980. Basic Principles of Membrane Transport. Cambridge University Press, Cambridge
21. Schwartz, J.H. 1976. H^+ current responses to CO_2 and carbonic anhydrase inhibition in turtle urinary bladder. *Am. J. Physiol.* **231:**565–572
22. Schwartz, J.H., Bethencourt, D., Rosen, S. 1982. Specialized function of the carbonic-anhydrase-rich and granular cells of turtle bladder. *Am. J. Physiol.* **242:**F627–F633
23. Schwartz, J.H., Rosen, S., Steinmetz, P.R. 1972. Carbonic anhydrase function and the epithelial organization of H^+ secretion in turtle urinary bladder. *J. Clin. Invest.* **51:**2653–2662
24. Schwartz, J.H., Tripolone, M. 1983. Intracellular pH of granular and mitochondria rich cells of turtle bladder. *Kidney Int.* **23:**239
25. Steinman, R.M., Mellman, I.S., Muller, W.A., Cohn, Z.A. 1983. Endocytosis and the recycling of plasma membrane. *J. Cell. Biol.* **96:**1–27
26. Steinmetz, P.R. 1974. Cellular mechanisms of urinary acidification. *Physiol. Rev.* **54:**890–956
27. Stetson, D.L., Steinmetz, P.R. 1983. Role of membrane fusion in CO_2 stimulation of proton secretion by turtle bladder. *Am. J. Physiol.* **245:**C113–C120
28. Stetson, D.L., Steinmetz, P.R. 1985. α and β types of carbonic anhydrase-rich cells in turtle bladder. *Am. J. Physiol.* **249:**F553–F565
29. Weibel, E.R. 1979. Stereological Methods. Vol. 1: Practical Methods for Biological Morphometry. Academic, London

Received 10 April 1986; revised 11 August 1986